Square-Planar and Butterfly Tetranuclear Ruthenium Clusters Incorporating the Doubly Linked Bis(dimethylsilylcyclopentadienyl) Ligand

David P. Klein, Maxim V. Ovchinnikov, Arkady Ellern,† and Robert J. Angelici*

Department of Chemistry, Iowa State University, Ames, Iowa 50011

Received May 2, 2003

The doubly linked dicyclopentadienyl complex $\{(\eta^5\text{-}C_5H_3)_2(SiMe_2)_2\}Ru_2(CO)_4$ (**1**) reacts with H_2 in benzene under broad-spectrum UV−visible photolysis ($254 < \lambda_{irr} < 600$ nm) to give the dinuclear $\{(\eta^5\text{-}C_5H_3)_2(SiMe_2)_2\}Ru_2(CO)_4H_2$ (**2**) and the tetranuclear clusters $\{(\eta^5\text{-}C_5H_3)_2(SiMe_2)_2\}_2Ru_4(CO)_3H_4$ (**3**) with a butterfly structure and $\{(\eta^5\text{-}C_5H_3)_2(SiMe_2)_2\}_2Ru_4(CO)_4H_4$ (**4**) with a square-planar structure. The linked $\{(\eta^5\text{-}C_5H_3)_2(SiMe_2)_2\}$ ligand is essential for the formation of the tetranuclear clusters (**3** and **4**), as unlinked analogues, $Cp'_2Ru_2(CO)_4$, give only di- and trinuclear products. Wavelength-dependent photolysis studies suggest that the first step in the reaction of **1** with H_2 involves metal−metal bond cleavage, which is supported by the all-terminal CO ligand geometry of **1**, the independent synthesis of **2**, and its photochemical reaction in the presence of H_2 to give **3** and **4**.

Introduction

Of the photochemical reactions of group 8 cyclopentadienyl dimers $[Cp'M(CO)_2]_2$ (M = Fe, Ru; Cp′ = η^5-C_5H_5 (Cp), η^5-C_5Me_5 (Cp*), C_5H_4Me), those of $[Cp'Fe(CO)_2]_2$ are extensive, but much less attention has been paid to the photochemistry of the ruthenium derivative.[1] Of particular relevance to the work reported in this paper are the photochemical reactions of $[Cp'Ru(CO)_2]_2$ (Cp′ = Cp, Cp*) and their derivatives with H_2. Knox and co-workers[2] reported that UV irradiation at 25 °C of toluene solutions of $Cp_2Ru_2(CO)_3(\mu\text{-CHR})$ (R = H, Me, CO_2Et) under a constant H_2 flow (1 atm) results in the formation of $Cp_3Ru_3H_3(CO)_3$. Shortly thereafter, the same group reported the synthesis of $Cp^*_2Ru_2(CO)_2H_2$ and $Cp^*_2Ru_2(CO)H_2$ with bridging hydride ligands by the UV photolysis of $Cp^*_2Ru_2(CO)_4$ in the presence of dihydrogen.[3] Bitterwolf and co-workers recently showed that photolysis of $Cp_2Ru_2(CO)_4$ in the presence of dihydrogen (10−20 bar) gives rise to the formation of $CpRu(CO)_2H$ by a process that involves CO loss, followed by oxidative addition of hydrogen.[4] Bitterwolf and co-workers[5] have also studied the photolysis of dimer systems with a single linking group $\{(\eta^5\text{-}C_5H_4)_2(Linker)\}Ru_2(CO)_4$ (Linker = CH_2, $C(CH_3)_2$, C_2H_4, and $Si(CH_3)_2$) in benzene/$CHCl_3$ or benzene/CH_2Cl_2 solvent mixtures, but there has been no analysis of the photochemical reactions of these singly linked systems with H_2.

Scheme 1

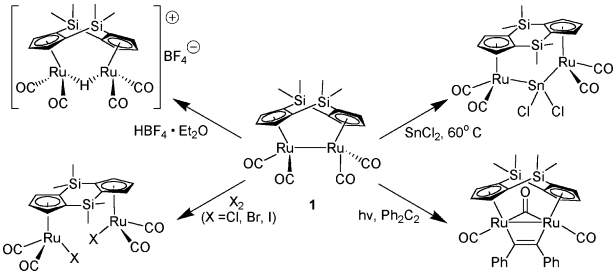

Recently, our group reported the synthesis and reactivity of the doubly linked dicyclopentadienyl diruthenium complex $\{(\eta^5\text{-}C_5H_3)_2(SiMe_2)_2\}Ru_2(CO)_4$ (**1**, Scheme 1).[6−8] Complex **1** reacts with H^+, halogens, and $SnCl_2$, in the same manner as $Cp_2Ru_2(CO)_4$ (Scheme 1). On the other hand, the doubly linked dicyclopentadienyl ligand has a dramatic effect on the photochemical reaction of **1** with diphenylacetylene, which gives $\{(\eta^5\text{-}C_5H_3)_2(SiMe_2)_2\}Ru_2(CO)_2(\mu\text{-CO})\{\eta^1\text{:}\eta^1\text{-}\mu_2\text{-C(Ph)C(Ph)}\}$ as one of three products; all of these products are different from those obtained in the photolysis of $Cp_2Ru_2(CO)_4$ with diphenylacetylene.[9] Herein, we report the reaction of **1** with H_2 under UV photolysis conditions to give the dinuclear dihydride $\{(\eta^5\text{-}C_5H_3)_2(SiMe_2)_2\}Ru_2(CO)_4H_2$ (**2**), the butterfly tetranuclear ruthenium cluster $\{(\eta^5\text{-}C_5H_3)_2(SiMe_2)_2\}_2Ru_4(CO)_3H_4$ (**3**), and the first square-planar cluster containing ruthenium and cyclopentadienyl ligands, $\{(\eta^5\text{-}C_5H_3)_2(SiMe_2)_2\}_2Ru_4(CO)_4H_4$ (**4**). The role of the doubly linked cyclopentadienyl ligand in the formation of the clusters and the mechanism for their formation are also investigated.

* To whom correspondence should be addressed. E-mail: angelici@iastate.edu.
† Iowa State University, Molecular Structure Laboratory.

(1) (a) Bitterwolf, T. E. *Coord. Chem. Rev.* **2000**, *206−207*, 419. (b) Meyer, T. J.; Caspar, J. V. *Chem. Rev.* **1985**, *85*, 187. (c) Wrighton, M. *Chem. Rev.* **1974**, *74*, 401.
(2) Forrow, N. J.; Knox, S. A. R.; Morris, M. J.; Orpen, A. G. *J. Chem. Soc., Chem. Commun.* **1983**, 234.
(3) Forrow, N. J.; Knox, S. A. R. *J. Chem. Soc., Chem. Commun.* **1984**, 679.
(4) Bitterwolf, T. E.; Linehan, J. C.; Shade, J. E. *Organometallics* **2000**, *19*, 4915.
(5) Bitterwolf, T. E.; Shade, J. E.; Hansen, J. A.; Rheingold, A. L. *J. Organomet. Chem.* **1996**, *514*, 13.
(6) Ovchinnikov, M. V.; Angelici, R. J. *J. Am. Chem. Soc.* **2000**, *122*, 6130.
(7) Ovchinnikov, M. V.; Guzei, I. A.; Angelici, R. J. *Organometallics* **2001**, *20*, 691.
(8) Ovchinnikov, M. V.; Wang, X.; Schultz, A. J.; Guzei, I. A.; Angelici, R. J. *Organometallics* **2002**, *21*, 3292.
(9) Knox, S. A. R.; Macpherson, K. A.; Orpen, A. G.; Rendle, M. C. *J. Chem. Soc., Dalton Trans.* **1989**, 1807.

10.1021/om0303247 CCC: $25.00
Publication on Web 08/01/2003

Scheme 2

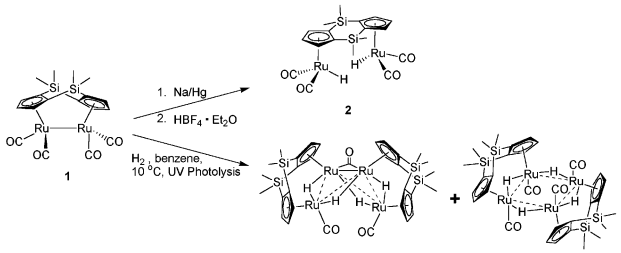

Results and Discussion

Synthesis of $\{(\eta^5\text{-}C_5H_3)_2(SiMe_2)_2\}Ru_2(CO)_4(H)_2$, 2. The reaction of complex **1** with Na/Hg amalgam produces the dianion $[\{(\eta^5\text{-}C_5H_3)_2(SiMe_2)_2\}Ru_2(CO)_4]^{2-}$,[10] which reacts with 2 equiv of $HBF_4{\cdot}OEt_2$ in THF to give **2** in 60% yield (Scheme 2).[11] The infrared spectrum of **2** in CH_2Cl_2 shows two strong ν(CO) bands at 2026 and 1965 cm^{-1}, on average 10 cm^{-1} higher than those of **1** and within 1 cm^{-1} of those in $CpRu(CO)_2H$.[12] The ^1H NMR spectrum of **2** in C_6D_6 shows a doublet at 4.77 ppm and a triplet at 5.15 ppm for the Cp protons and two resonances for the methyl groups on the silicon bridge at 0.09 and 0.46, indicating the presence of two mirror planes within the complex. The ^1H NMR spectrum exhibits a hydride signal at −10.41 ppm, 0.3 ppm lower than that of $CpRu(CO)_2H$.[12]

Reaction of $\{(\eta^5\text{-}C_5H_3)_2(SiMe_2)_2\}Ru_2(CO)_4$ (1) with Dihydrogen. Complex **1** reacts with molecular hydrogen (1 atm) in benzene at 10 °C under UV photolysis to give the tetranuclear ruthenium complexes **3** and **4** (Scheme 2). After column chromatography on alumina with hexanes−CH_2Cl_2, the black complex **3** and the purple **4** are isolated as slightly air-sensitive solids in 4% and 38% yield, respectively. The ^1H NMR and IR spectra of the reaction mixture also show the presence of **2** and other ruthenium-containing products; however, their isolation and characterization were unsuccessful.

The IR spectrum of complex **3** in hexanes shows a strong ν(CO) band at 1949 cm^{-1} and a medium ν(CO) band at 1758 cm^{-1}, which may be assigned to terminal and bridging CO ligands, respectively. The ^1H NMR spectrum of complex **3** shows four sets of multiplets in the Cp region, and also four methyl resonances at 0.20, 0.32, 0.49, and 0.61 ppm, which indicates that there are no mirror planes in the $(\eta^5\text{-}C_5H_3)_2(SiMe_2)_2$ ligands. Complex **3** also exhibits two hydride resonances at −18.00 and −15.38 ppm, both of which are triplets, indicating two distinct bridging hydride environments and the absence of rapid interchange between the two hydride sites. The ^{13}C NMR spectrum shows nine resonances for the 10 different carbons on the Cp groups, with two peaks overlapping to give one signal. Signals for the carbon monoxide ligands could not be identified due to the low solubility of the complex.

The molecular structure of **3**, determined by X-ray diffraction (Figure 1, Table 1), shows the butterfly arrangement of the ruthenium atoms. The butterfly has a fold angle of 109.5°, defined as the angle between

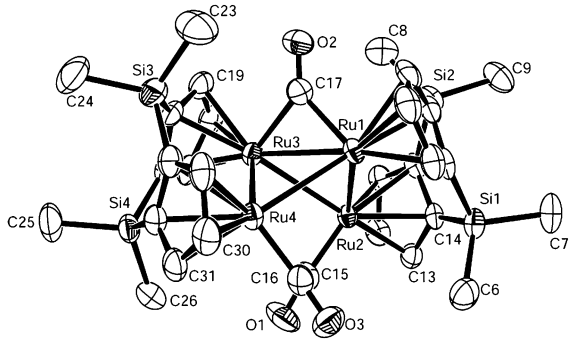

Figure 1. Thermal ellipsoid drawing of $\{(\eta^5\text{-}C_5H_3)_2(SiMe_2)_2\}_2Ru_4(CO)_3H_4$ (**3**) with 50% ellipsoid probability and labeling scheme. Hydrogen atoms are omitted for clarity. Bridging hydride ligands reside on the following Ru−Ru bonds: Ru(1)−Ru(2), Ru(2)−Ru(3), Ru(3)−Ru(4), and Ru(1)−Ru(4). Selected bond distances (Å) and angles (deg): Ru(1)−Ru(2), 2.927(1); Ru(2)−Ru(3), 3.002(1); Ru(1)−Ru(3), 2.789 (1); Ru(3)−Ru(4), 2.926 (1); Ru(1)−Ru(4), 3.017 (1); Ru(1)−C(17), 2.017(6); Ru(3)−C(17), 2.021(6); Ru(2)−C(15), 1.836(7); C(17)−O(2), 1.171(7); C(15)−O(1), 1.151-(7); Ru(1)−Cp(centroid), 1.836; Ru(2)−Cp(centroid), 1.875; Ru(3)−Cp(centroid), 1.827; Ru(4)−Cp(centroid), 1.885; ∠Ru-(1)−Ru(3)−Ru(4) 63.66; ∠Ru(1)−Ru(3)−Ru(2) 60.6; ∠Ru-(3)−Ru(4)−Ru(1) 55.96; ∠Ru(3)−Ru(1)−Ru(4) 60.37; ∠Ru(3)−Ru(1)−Ru(2) 63.29; ∠Ru(1)−Ru(2)−Ru(3) 56.11; ∠Cp(centroid)−Ru(1)−Ru(2)−Cp(centroid), 17.7; ∠Cp(centroid)−Ru(3)−Ru(4)−Cp(centroid), 16.7; ∠Butterfly 109.5; ∠Cp−Cp fold angle, 127.8.

Ru(2), the Ru(1)−Ru(3) bond centroid, and Ru(4). The butterfly contains three discrete types of metal−metal bonds, with two types bridged by a hydride ligand. Although the hydride ligands were not located in the X-ray structure, the two upfield doublets in the ^1H NMR spectrum suggest that the four hydride ligands are located on the metal−metal bonds that do not have a bridging CO ligand. The CO-bridged Ru(1)−Ru(3) bond with a bond distance of 2.789 Å is 0.05 Å longer than that in the carbonyl-bridged $Cp_2Ru_2(CO)_4$ (2.735(2) Å).[13] The Ru(1)−Ru(2) and Ru(3)−Ru(4) bonds that are bridged by $(\eta^5\text{-}C_5H_3)_2(SiMe_2)_2$ and hydride ligands have an average distance of 2.93 Å. This distance is 0.10 Å longer than that in **1** (2.8180(3) Å),[10] due to the presence of the bridging hydride ligand, and it is 0.19 Å shorter than that in **1-H**$^+$ (3.103(3) Å).[14] The hydride-bridged metal−metal bonds that are not bridged by the $(\eta^5\text{-}C_5H_3)_2(SiMe_2)_2$ ligand, Ru(2)−Ru(3) and Ru(1)−Ru(4), have an average distance of 3.01 Å, which is 0.05 Å longer than the hydride-bridged Ru−Ru bonds in $Cp_3Ru_3H_3(CO)_3$[2] and 0.09 Å longer than the Ru(1)−Ru(2) and Ru(3)−Ru(4) bonds that have both hydride and $(\eta^5\text{-}C_5H_3)_2(SiMe_2)_2$ bridges. Thus, the Ru−Ru distances in **3** increase in the order Ru(1)−Ru(3) (2.79 Å, CO-bridged) < Ru(1)−Ru(2), Ru(3)−Ru(4), (2.93 Å, hydride- and $(\eta^5\text{-}C_5H_3)_2(SiMe_2)_2$-bridged) < Ru(2)−Ru(3), Ru(1)−Ru(4) (3.01 Å, hydride-bridged).

The IR spectrum of **4** in hexanes exhibits a single very strong ν(CO) band at 1946 cm^{-1}, indicating the presence of only terminal CO ligands. In the ^1H NMR spectrum of **4**, all of the cyclopentadienyl rings are equivalent, but each of the three protons on the rings differ, which

(10) Ovchinnikov, M. V.; Klein, D. P.; Guzei, I. A.; Choi, M.-G.; Angelici, R. J. *Organometallics* **2002**, *21*, 617.
(11) Cheng, T.; Bullock, R. M. *Organometallics* **2002**, *21*, 2325.
(12) Kazlauskas, R. J.; Wrighton, M. S. *Organometallics* **1982**, *1*, 602.
(13) Mills, D. S.; Nice, J. P. *J. Organomet. Chem.* **1967**, *9*, 339.
(14) Ovchinnikov, M. V.; Wang, X.; Schultz, A. J.; Guzei, I. A.; Angelici, R. J.; *Organometallics* **2002**, *21*, 3292.

Table 1. Crystal Data and Structure Refinement for 3 and 4

	3	4
empirical formula	$C_{31}H_{40}O_3Ru_4Si_4 \cdot C_4H_{10}O$	$C_{32}H_{40}O_4Ru_4Si_4 \cdot 2C_4H_{10}O$
fw	1051.39	1153.52
temperature	298(2) K	173(2) K
wavelength	0.71073 Å	0.71073 Å
cryst syst	monoclinic	rhombohedral
space group	*P*2(1)/*n*	*R*-3
unit cell dimens	$a = 15.389(6)$ Å $b = 18.223(7)$ Å $c = 15.695(6)$ Å $\alpha = 90°$ $\beta = 115.553(5)°$ $\gamma = 90°$	$a = 17.8969(16)$ Å $b = 17.8969(16)$ Å $c = 17.8969(16)$ Å $\alpha = 114.8090(10)°$ $\beta = 114.8090(10)°$ $\gamma = 114.8090(10)°$
volume	3971(3) Å^3	3263.3(5) Å^3
Z	4	3
density(calcd)	1.752 Mg/m^3	1.758 Mg/m^3
abs coeff	1.648 mm^{-1}	1.516 mm^{-1}
F(000)	2080	1734
cryst size	0.3 × 0.3 × 0.1 mm^3	0.3 × 0.3 × 0.2 mm^3
θ range for data collection	1.82 to 24.81°	1.81 to 28.27°
index ranges	$-18 \le h \le 18$, $-21 \le k \le 21$ $-18 \le l \le 18$	$-22 \le h \le 22$, $-23 \le k \le 23$, $-23 \le l \le 22$
no. of reflns collected	28 854	29 237
no. of ind reflns	6839 [*R*(int) = 0.0727]	5219 [*R*(int) = 0.0205]
abs corr	empirical, multiscan	empirical, multiscan
no. of data/ restraints/ params	6839/0/434	5219/4/225
goodness-of-fit on F^2	0.986	1.037
final *R* indices [$I > 2\sigma(I)$]	R1 = 0.0433, wR2 = 0.1095	R1 = 0.0239, wR2 = 0.0653
R indices (all data)	R1 = 0.0576, wR2 = 0.1187	R1 = 0.0290, wR2 = 0.0683
largest diff peak and hole	1.662 and −1.371 e Å^{-3}	0.852 and −0.772 e Å^{-3}

gives rise to the three resonances at 5.00, 5.13, and 5.25 ppm. The peak at 5.13 ppm is a triplet, due to coupling to the two adjacent protons; however, the resonances at 5.00 and 5.25 ppm are multiplets. The COSY spectrum in the Cp region shows that these multiplets result from a small amount of coupling between the protons on opposite sides of the Cp ring. In each $(\eta^5\text{-}C_5H_3)_2(SiMe_2)_2$ ligand, the four methyl groups on silicon are all inequivalent, with resonances observed at 0.47, 0.43, 0.36, and 0.25 ppm. Two hydride resonances occur at −19.95 and −20.33 ppm, which indicates that rapid exchange does not occur between the hydride sites. The ^{13}C NMR spectrum has the expected four resonances for the methyl groups as well as five signals for the five inequivalent C_5H_3 carbon atoms. The signal for the four equivalent CO ligands appears at 205.72 ppm.

The molecular structure of complex **4** has been determined by X-ray crystallography and is the first known example of a cyclopentadienyl-containing square-planar ruthenium complex (Figure 2). The complex has a square-planar Ru_4 core, as is illustrated by the fact that all of the angles in the square deviate from 90° by no more than ±0.2%, or 0.11°, and the planarity of the Ru atoms is confirmed by a 0° torsion angle for ∠Ru(1)−Ru(2A)−Ru(1A)−Ru(2). The presence of four metal−metal bonds and four hydride ligands, coupled with the presence of an inversion center, necessitates a bridging hydride ligand on every metal−metal bond in **4**. At 3.1107(4) Å, the hydride-bridged metal−metal bond distance between two ruthenium atoms, Ru(1)−Ru(2), sharing one $(\eta^5\text{-}C_5H_3)_2(SiMe_2)_2$ ligand is roughly 0.18 Å longer than the average of analogous bonds in **3** (2.93 Å for Ru(1)−Ru(2) and Ru(3)−Ru(4)). The metal−metal bonds with only a bridging hydride, Ru(1)−Ru(2A) or Ru(2)−Ru(1A), have a bond distance of 3.0991(4) Å, 0.08 Å longer than the average of similar bond lengths in **3** (3.01 Å for Ru(1)−Ru(4) and Ru(2)−Ru(3)). The CO ligands on Ru(1) and Ru(2) are almost exactly eclipsed, as indicated by a 2.6° torsion angle for C(16)−Ru(1)−Ru(2)−C(15).

The composition of complex **3** differs from that of **4** by only one carbon monoxide ligand. The electron count in **3** is 62 e$^-$, which is consistent with a butterfly structure, while the 64 e$^-$ count for **4** is consistent with a square-planar structure.[15] In an attempt to convert **3** into **4**, CO was bubbled through THF solutions of **3** at room temperature or at 60° C, but there was no reaction. Likewise, conversion of **4** to **3** by removal of CO did not occur by bubbling Ar through refluxing benzene solutions of **4** or by photolysis of **4** in benzene under a constant Ar flow. A possible reason for this lack of interconversion is the relative positions of the two $(\eta^5\text{-}C_5H_3)_2(SiMe_2)_2$ ligands in **3** and **4**. If the Ru(1)−Ru(3) bond in **3** were cleaved to form a square plane of ruthenium atoms, the $(\eta^5\text{-}C_5H_3)_2(SiMe_2)_2$ ligands would lie on the same side of this plane. However, the $(\eta^5\text{-}C_5H_3)_2(SiMe_2)_2$ ligands in **4** actually reside on opposite sides of the plane. Thus, further bond cleavage would be required to achieve the structure of **4**. The lack of interconversion between **3** and **4** indicates that **3** and **4** are formed (Scheme 3) by different pathways.

Proposed Mechanism for the Formation of Clusters 3 and 4. On the basis of experiments described below, we propose a mechanism (Scheme 3) for the formation of clusters **3** and **4** from **1** and H_2 under UV photolysis (Scheme 2). The first step (*A*) in the mechanism is the photolytic cleavage of the Ru−Ru bond in **1** to give a diradical which reacts (step *B*) with H_2 to give **2**. Indeed, **2** seems to be an important intermediate in the formation of the clusters, as it can be observed spectroscopically (IR, ^1H NMR) in samples taken during the course of the photolytic reaction of **1** and H_2; it is also present in small amounts at the end of the reaction. Furthermore, when independently synthesized **2** is photolyzed in a benzene solution under a constant H_2 flow, clusters **3** and **4** are the only observed products. When the same photolytic reaction of **2** is done in the presence of Ar instead of H_2, only **1** and small amounts of **3** and **4** are observed in the ^1H NMR spectrum. The large amount of **1** recovered at the end of the reaction suggests a secondary photolytic reaction of **2** with loss of H_2 to give **1**, similar to the reaction of $CpRu(CO)_2H$ under UV photolysis conditions ($260 < \lambda_{irr} < 400$ nm) to give the $CpRu(CO)_2^\bullet$ radical and H_2.[16]

Step *C* in Scheme 3 involves the loss of two CO ligands to give intermediate **5**, consistent with recent results from Bitterwolf and co-workers,[16] who have shown that photolysis ($260 < \lambda_{irr} < 400$ nm) of $CpRu(CO)_2H$ in frozen Nujol matrixes results in the loss of CO to give [CpRu(CO)H], $[CpRu(CO)_2^\bullet]$, and $[(\eta^4\text{-}C_5H_6)Ru(CO)_2]$. Photolytic loss of an additional CO from **5**

(15) Cotton, F. A., Wilkinson, G., Murillo, C. A., Bochman, M., Eds. *Advanced Inorganic Chemistry*, 6th ed.; John Wiley and Sons: New York, 1999; p 661.

(16) Bitterwolf, T. E.; Linehan, J. C.; Shade, J. E. *Organometallics* **2001**, *20*, 775.

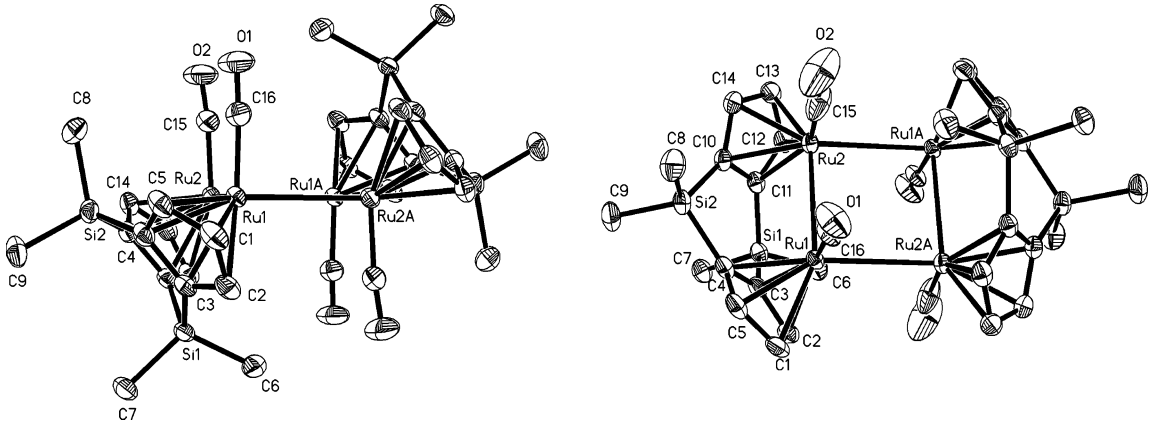

Figure 2. Thermal ellipsoid drawing of $\{(\eta^5\text{-}C_5H_3)_2(SiMe_2)_2\}_2Ru_4(CO)_4H_4$ (**4**) with 50% ellipsoid probability and labeling scheme. Hydrogen atoms are omitted for clarity. Bridging hydride ligands reside on all Ru−Ru bonds. Selected bond distances (Å) and angles (deg): Ru(1)−Ru(2), 3.1107(4); Ru(1)−Ru(2A), 3.0991(4); Ru(1)−C(16), 1.834(3); Ru(2)−C(15), 1.825(3); C(16)−O(1), 1.152(3); C(15)−O(2), 1.151(4); Ru(1)−Cp(centroid), 1.870; Ru(2)−Cp(centroid), 1.871; ∠Ru(1)−Ru(2)−Ru(1A), 89.89; ∠Ru(2)−Ru(1A)−Ru(2A), 90.11; ∠Ru(1A)−Ru(2A)−Ru(1), 89.89; ∠Ru(2A)−Ru(1)−Ru(2), 90.11; ∠Cp(centroid)−Ru(1)−Ru(2)−Cp(centroid), 1.6; ∠Cp−Cp fold angle, 129.6.

Scheme 3

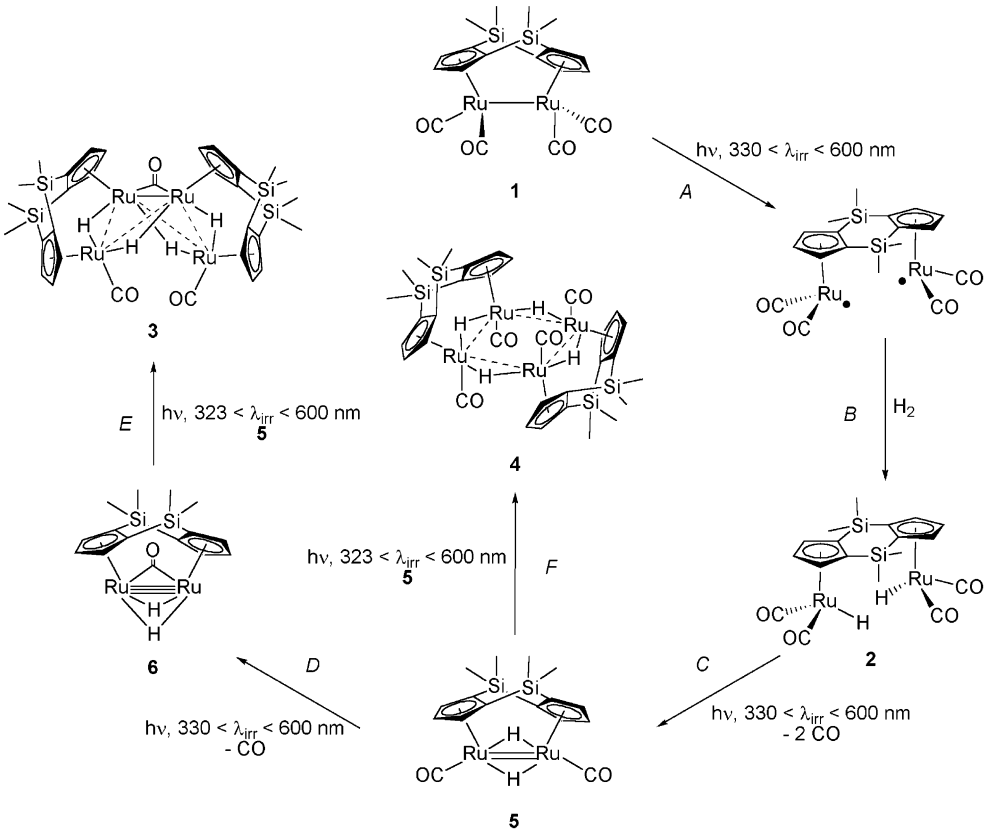

would give **6** (step *D*). There are precedents in the literature[3,17] for the existence of analogues of **5** and **6**, as well as for the conversion of **5** to **6**. Forrow and Knox[3] showed that photolysis of $Cp^*_2Ru_2(CO)_4$ in the presence of 1 atm of H_2 gives the trans-Cp complex $Cp^*_2Ru_2(CO)_2H_2$ and $Cp^*_2Ru_2(CO)H_2$ as products, analogues of **5** and **6**. Independently synthesized $Cp^*_2Ru_2(CO)_2H_2$ undergoes loss of CO during UV photolysis to give $Cp^*_2Ru_2(CO)H_2$.[3] Although **5** and **6** could not be isolated and completely characterized, the presence of hydride intermediates, consistent with the proposed structures of **5** and **6**, can be seen in the ^{1}H NMR spectrum of the reaction solution with hydride resonances at −19.9 and −17.3 ppm. The hydride resonances for **5** and **6** in C_6D_6 are in the same region as those for $Cp^*_2Ru_2(CO)_2H_2$ (−17.4 ppm) and $Cp^*_2Ru_2(CO)H_2$ (−13.7 ppm).[3] In the final steps of the mechanism, **5** reacts with **6** to give the butterfly cluster **3** (step *E*), and **5** dimerizes (step *F*) to form the square-planar **4**. A related dimerization has been observed for other ruthenium hydride clusters,[18] but the reaction is blocked for $Cp^*_2Ru_2(CO)_2H_2$

(17) Mahmoud, K. A.; Rest, A. J.; Alt, H. G. *J. Chem. Soc., Dalton Trans.* **1985**, 1365.

(18) Cabeza, J. A.; Fernándes-Colinas, J. M.; García-Granda, S.; Llamazares, A.; López-Ortíz, F.; Riera, V.; Van der Maelen, J. F. *Organometallics* **1994**, *13*, 426.

Scheme 4

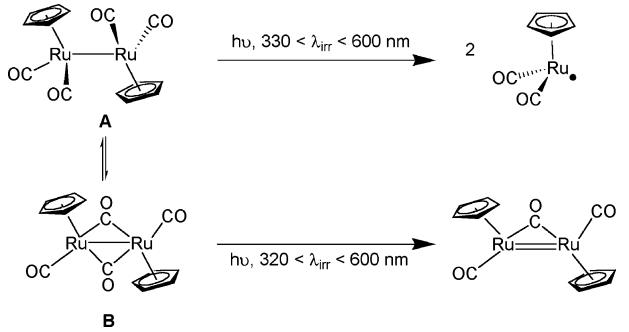

and $Cp^*_2Ru_2(CO)H_2$ due to steric and electronic properties of the Cp* ligands.

Photochemical Details of the Proposed Mechanism. A key step in the mechanism (Scheme 3) is the initial photolytic activation of **1** (step *A*). Two possible pathways for the photoactivation of $Cp'_2Ru_2(CO)_4$ dimers are shown in Scheme 4. The pathway taken depends on whether the dimer contains bridging CO ligands or not.[19] As is well known,[20] $Cp_2Ru_2(CO)_4$ exists as an equilibrium mixture of nonbridged (**A**) and bridged (**B**) structures. In the electronic spectra of both isomers **A** and **B**, the main spectral feature is a band attributed to the promotion of an electron from the metal−metal bonding orbital to the metal−metal antibonding orbital, $\sigma_b \rightarrow \sigma^*$. If $Cp_2Ru_2(CO)_4$ contains no bridging CO ligands, as in **A**, then the $\sigma_b \rightarrow \sigma^*$ band occurs at ∼330 nm;[20] when **A** is photolyzed ($330 < \lambda_{irr} < 600$ nm) in nonpolar solvents, the products observed are $CpRu(CO)_2^\bullet$ radicals, resulting from homolysis of the metal−metal bond.[19] In isomer **B**, the $\sigma_b \rightarrow \sigma^*$ band is at ∼265 nm;[20] when frozen inert gas matrixes of **B** at 12 K are photolyzed with UV light ($320 < \lambda_{irr} < 390$ nm), the main product observed is one resulting from CO loss, $[Cp_2Ru_2(CO)_3]$.[21]

The solid-state structure of **1**, determined by X-ray crystallography, shows that all four CO ligands are in terminal positions, and the infrared spectrum of **1** in solution, regardless of solvent polarity, shows no sign of bridging CO ligands.[10] The UV−visible spectrum of **1** in THF exhibits a λ_{max} at ∼355 nm (Figure 3), which can be attributed to the $\sigma_b \rightarrow \sigma^*$ transition. On the basis of the all-terminal geometry of the CO ligands in **1** and the location of the $\sigma_b \rightarrow \sigma^*$ transition in the UV−visible spectrum, one expects the initial photolytic reaction to involve cleavage of the Ru−Ru bond to give the diradical intermediate in Scheme 3 (step *A*).

If the initial photoprocess were loss of CO as in $Cp_2Ru_2(CO)_4$, isomer **B**, the generated intermediate would be $[\{(\eta^5\text{-}C_5H_3)_2(SiMe_2)_2\}Ru_2(CO)_3]$ (**7**). The absence of **7** as an intermediate in the reaction of **1** and H_2 is indicated by the fact that photolysis of benzene solutions of **1** in the presence of phosphines, PR_3, does not lead to formation of complexes of the type $\{(\eta^5\text{-}C_5H_3)_2(SiMe_2)_2\}Ru_2(CO)_3PR_3$; however, these phosphine-substituted complexes can be synthesized by thermal reactions of **1** with phosphines at 200 °C.[10] Intermediate **7**, if present, would also be expected to react in the presence of H_2/CO mixtures to give only **1**. However, if benzene solutions of **1** are photolyzed in the presence of H_2 and CO (1:1), the product is not **1**, but is instead **2**, resulting from Ru−Ru bond homolysis. Therefore, it appears that CO loss from **1** is not involved in the photolytic synthesis of **3** and **4** from **1** and H_2.

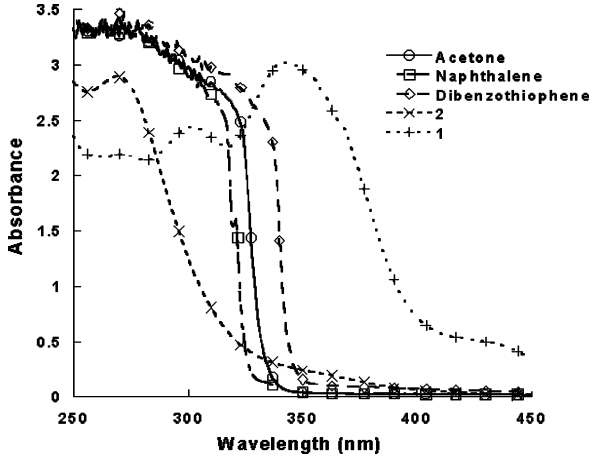

Figure 3. UV−visible spectra of acetone, 7.8 mM naphthalene in benzene, 76 mM DBT in benzene, 2.0 mM **2** in THF, and 0.34 mM **1** in THF.

During the synthesis of **3** and **4**, it was noticed that yields of the clusters were much higher when benzene was used as the solvent rather than THF. A comparison of the UV−visible spectra of **1** in benzene and in THF shows that benzene completely absorbs all light with wavelengths less than 250 nm; therefore, the benzene solvent acts as an internal filter that removes high-energy light that leads to decomposition and formation of precipitates. The spectrum of **1** in THF (Figure 3) shows a λ_{max} at ∼355 nm, as well as two other peaks at ∼300 and ∼275 nm. In contrast, the spectrum for **2** shows a peak at 270 nm and a broad shoulder on the high-wavelength side of the peak. The shoulder peak is assigned to the energy required to remove CO ligands from **2**, on the basis of experiments described below.

To understand the dependence of the reaction on different wavelengths of light, the broad-spectrum UV−vis light source was filtered using solutions of dibenzothiophene (DBT), acetone, and naphthalene.[22] Photolysis of **1** and H_2 in benzene for 24 h using the DBT filter, which allows light with wavelengths greater than 342 nm ($342 < \lambda_{irr} < 600$ nm)[23] to reach the reaction solution, resulted in no apparent reaction. Since only **1** was recovered at the end of the reaction, the most energetic light near 342 nm is not sufficient to remove CO from **2** (step *C*). Photolysis under the same conditions, but with an acetone filter solution ($330 < \lambda_{irr} < 600$ nm), resulted in the formation of **2**, **5**, and **6**, as observed in the ^{1}H NMR spectrum of the reaction solution, but complexes **3** and **4** were not observed.

(19) (a) Macyk, W.; Herdegen, A.; Karocki, A.; Stochel, G.; Stasicka, Z.; Sostero, S.; Traverso, O. *J. Photochem. Photobiol. A* **1997**, *103*, 221. (b) Macyk, W.; Herdegen, A.; Stochel, G.; Stasicka, Z.; Sostero, S.; Traverso, O. *Polyhedron* **1997**, *16*, 3339. (c) Sostero, S.; Rehorek, D.; Polo, E.; Traverso, O. *Inorg. Chem. Acta* **1993**, *209*, 171.

(20) Abrahamson, H. B.; Palazzotto, M. C.; Reichel, C. L.; Wrighton, M. S. *J. Am. Chem. Soc.* **1979**, *101*, 4123.

(21) Bloyce, P. E.; Campen, A. K.; Hooker, R. H.; Rest, A. J.; Thomas, N. R.; Bitterwolf, T. E.; Shade, J. E. *J. Chem. Soc., Dalton Trans.* **1990**, 2833.

(22) Freedman, D. A.; Gill, T. P.; Blough, A. M.; Koefod, R. S.; Mann, K. R. *Inorg. Chem.* **1997**, *36*, 95.

(23) The cutoff point is defined as the wavelength where absorbance of the filter solution is 1.0: Lambert, J. B.; Shurvell, H. F.; Lightner, D. A.; Cooks, R. G. *Organic Structural Spectroscopy*, 1st ed.; Prentice Hall: New Jersey, 1998; p 270.

Formation of **2**, **5**, and **6** is the result of the acetone filter solution allowing energy into the reaction that is sufficient to promote steps *A*, *C*, and *D*, but not steps *E* and *F*. When a naphthalene filter ($323 < \lambda_{irr} < 600$ nm) was used, the ^{1}H NMR spectrum of the reaction solution showed the presence of **2**, **3**, **4**, **5**, and **6**, as there is enough energy to cause all of the photolytic reactions in Scheme 3. When the reaction time was extended from 24 to 72 h, the naphthalene-filtered photolysis of **1** with H_2 resulted in complete conversion to clusters **3** and **4**, in 12% and 74% isolated yields, respectively. The results of the filtering experiments show that, in order for the clusters to form, light with wavelengths between 323 and 600 nm must be allowed into the reaction. The energy contained in this light must be great enough to cleave the metal−metal bond (step *A*), eject CO groups from **2** and **5** (steps *C* and *D*), and promote the dimerizations of **5** and **6** (steps *E* and *F*).

Conclusions

Photolysis of benzene solutions of $\{(\eta^5\text{-}C_5H_3)_2(SiMe_2)_2\}Ru_2(CO)_4$ (**1**) in the presence of 1 atm of H_2 leads to clusters $\{(\eta^5\text{-}C_5H_3)_2(SiMe_2)_2\}_2Ru_4(CO)_3H_4$ (**3**) and $\{(\eta^5\text{-}C_5H_3)_2(SiMe_2)_2\}_2Ru_4(CO)_4H_4$ (**4**). Formation of the tetraruthenium centers in **3** and **4** depends on the doubly linked $(\eta^5\text{-}C_5H_3)_2(SiMe_2)_2$ ligand, which keeps the two Ru atoms in close proximity, thereby favoring dimerization to the tetranuclear clusters. The molecular structure of **3** indicates that the ruthenium core exists as a butterfly structure containing three different types of Ru−Ru bonds. Complex **4** contains a Ru_4 core that exhibits the unusual square-planar geometry and is the first example of a square-planar complex containing both Ru and cyclopentadienyl ligands. Clusters **3** and **4** are proposed to be formed by a process that involves initial metal−metal bond cleavage (Scheme 3), which is followed by reaction with H_2 to form $\{(\eta^5\text{-}C_5H_3)_2(SiMe_2)_2\}Ru_2(CO)_4H_2$ (**2**). Complex **2** then undergoes photolytic loss of 2 or 3 CO ligands to give **5** and **6**, respectively, which dimerize to give complexes **3** and **4**. Attempts to interconvert complexes **3** and **4** were unsuccessful, which is consistent with their formation by different pathways.

Experimental Section

General Considerations. All reactions were carried out under an inert atmosphere of dry argon or nitrogen using standard Schlenk techniques. Diethyl ether, methylene chloride, and hexanes were purified on alumina using a Solv-Tek solvent purification system, similar to one reported by Grubbs.[24] Benzene was refluxed over and distilled from calcium hydride.[25] Hydrogen (Air Products) and carbon monoxide (Air Products) were used as received. $\{(\eta^5\text{-}C_5H_3)_2(SiMe_2)_2\}Ru_2(CO)_4$ (**1**) was prepared by the reported method.[6] All other chemicals were used as received from Aldrich. Alumina (neutral, activity I, Aldrich) was degassed under vacuum for 24 h at room temperature and treated with Ar-saturated distilled water (7.5% w/w). ^{1}H and ^{13}C NMR spectra were recorded on a Bruker DRX-400 spectrometer using deuterated solvents as internal references. Solution infrared spectra were recorded on a Nicolet-560 spectrometer using NaCl cells with a 0.1 mm path length. Elemental analyses were performed on a Perkin-Elmer 2400 series II CHNS/O analyzer or by Quantitative Technologies, Inc., Whitehouse, NJ. UV−visible spectra were recorded on an HP 8245 spectrometer, using 1 cm path length quartz cuvettes.

All photochemical reactions were carried out in 60 mL quartz Schlenk photolysis tubes fitted with a coldfinger condenser that is submersed in the reaction solution. A Hanovia 450 W medium-pressure Hg lamp with a quartz cooling jacket was used as the ultraviolet light source. The temperature of each reaction was controlled with an Isotemp 1013P refrigerated circulating bath (Fisher Scientific) with hoses connected to the coldfinger condenser. Filter solutions were 76 mM DBT in benzene, pure acetone, and 7.8 mM naphthalene in benzene.[22] The photolysis tube was immersed into a filter solution (average thickness of 1.5 cm) in a quartz beaker; the level of the reaction solution was below that of the filter solution.

Synthesis of $(CpSiMe_2)_2Ru_2(CO)_4H_2$, 2. A solution of **1** (50 mg, 0.090 mmol) in THF (10 mL) was added to Na/Hg (50 mg/2 mL).[10] The mixture was stirred for 1 h, and the resulting yellow-green solution was filter cannulated to a new flask. To this solution was added $HBF_4{\cdot}Et_2O$ (26 μL, 0.21 mmol). The solution was stirred for 1 h, after which the solvent was reduced to 2 mL under vacuum; then hexanes (15 mL) was added to precipitate $NaBF_4$. After filtration, solvent was removed under vacuum. The residue was dissolved in a minimum of hexanes and passed through a short alumina column (1 cm × 5 cm); **1** remained on the column, and pure **2** was collected with hexanes (25 mL) as the eluent. Concentrating the hexanes solution to near saturation, followed by cooling at −78° C, gave 23 mg of **2** (46%, based on Ru) after filtration. Solid **2** decomposes to **1** after 2−3 days in the dark under Ar at 0 °C, and 1 day at room temperature; it is much more stable under a H_2 atmosphere. Solutions of **2** decompose to **1** after approximately 8 h at room temperature. ^{1}H NMR (400 MHz, C_6D_6): δ −10.41 (s, 2 H, Ru-*H*), 0.09 (s, 6 H, Si(C*H*$_3$)), 0.46 (s, 6 H, Si(C*H*$_3$)), 4.77 (d, J = 2.4 Hz, 4 H), 5.15 (t, J = 2.4 Hz, 2 H). IR (benzene): ν(CO) (cm^{-1}) 2029 (vs), 1966 (vs). IR (CH_2Cl_2): 2026 (vs), 1965 (vs). Anal. Calcd for $C_{18}H_{20}O_4Ru_2Si_2$: C, 38.70; H, 3.61. Found: C, 39.21; H, 3.82.

Reaction of 1 with Hydrogen. To a quartz Schlenk tube were added 50 mg (0.09 mmol) of **1** and a stirbar. After benzene (30 mL) was added, the flask was equipped with a coldfinger condenser under Ar flow. A Teflon cannula was used to provide a slow steady stream of hydrogen through the solution, and the flask was purged with hydrogen for 10 min. The tube was then cooled to 10 °C, fitted with an oil bubbler, and irradiated for 48 h under a slow hydrogen flow. Then, the purple-black solution was filtered through a short pad of Celite (0.5 × 2 cm) and transferred to a new flask. The solvent was removed under vacuum, and the residue was dissolved in 10 mL of hexanes−CH_2Cl_2 (5:1). The mixture was then chromatographed on an alumina column (2 × 20 cm) first with hexanes−CH_2Cl_2 (10:1, 200 mL) and then with hexanes−CH_2Cl_2 (5:1) as the eluent. After collecting a purple band with hexanes−CH_2Cl_2 (5:1), a black band was eluted with hexanes−CH_2Cl_2 (4:1). Solvent was then removed from both fractions under vacuum. The first fraction yielded 17 mg of $\{(\eta^5\text{-}C_5H_3)_2(SiMe_2)_2\}_2Ru_4(CO)_4H_4$, **4** (38%, based on Ru). ^{1}H NMR (400 MHz, C_6D_6): δ −20.33 (t, J = 4.0 Hz, 2 H, Ru-*H*-Ru), −19.95 (t, J = 4.0 Hz, 2 H, Ru-*H*-Ru), 0.25 (s, 6 H, Si(C*H*$_3$)), 0.36 (s, 6 H, Si(C*H*$_3$)), 0.43 (s, 6 H, Si(C*H*$_3$)), 0.47 (s, 6 H, Si(C*H*$_3$)), 5.00 (m, 4 H, Cp *H*), 5.13 (t, J = 2.4 Hz, 4H, Cp *H*), 5.25 (m, 4 H, Cp *H*). ^{13}C NMR (100 MHz, C_6D_6): −3.76, −1.13, 2.94, 5.46 (Me); 79.09, 84.85, 88.76, 97.20, 98.57 (Cp); 205.72 (CO). IR (hexanes): ν(CO) (cm^{-1}) 1956 (vs). Anal. Calcd for $C_{32}H_{40}O_4Ru_4Si_4$: C, 38.23; H, 4.01. Found: C, 38.25; H, 4.02. The second fraction yielded 6 mg of $\{(\eta^5\text{-}C_5H_3)_2(SiMe_2)_2\}_2Ru_4(CO)_3H_4$, **3** (4%, based on Ru). ^{1}H NMR (400 MHz, C_6D_6): δ −18.00 (t, J = 2.9 Hz, 2 H, Ru-*H*-Ru), −15.38 (t, J = 2.9 Hz, 2 H, Ru-*H*-

(24) Pangborn, A. B.; Giardello, M. A.; Grubbs, R. H.; Rosen, R. K.; Timmers, F. J. *Organometallics* **1996**, *15*, 1518.

(25) Perrin, D. D.; Armarego, W. L. F.; Perrin, D. R. *Purification of Laboratory Chemicals*, 2nd ed.; Pergamon: New York, 1980.

Ru), 0.20 (s, 6 H, Si(CH_3)), 0.32 (s, 6 H, Si(CH_3)), 0.49 (s, 6 H, Si(CH_3)), 0.61 (s, 6 H, Si(CH_3)), 4.79 (m, 4 H, Cp *H*), 5.21 (m, 4 H, Cp *H*), 5.45 (m, 2 H, Cp *H*), 5.65 (m, 2 H, Cp *H*). ^{13}C NMR (100 MHz, C_6D_6): −3.12, −1.75, 1.37, 4.01 (Me); 81.54, 82.05, 84.11, 87.41, 89.65, 91.77, 96.93, 97.18, 106.27 (Cp). IR (hexanes): ν(CO) (cm^{-1}) 1949 (vs), 1758 (m). Anal. Calcd for $C_{31}H_{40}O_3Ru_4Si_4$: C, 38.10; H, 4.13. Found: C, 38.45; H, 3.90.

Synthesis of {(η^5-C_5H_3)$_2$($SiMe_2$)$_2$}$_2$$Ru_4(CO)_3$$H_4$ (3) and {(η^5-C_5H_3)$_2$($SiMe_2$)$_2$}$_2$$Ru_4(CO)_4$$H_4$ (4). Complex **1** (50 mg, 0.09 mmol) and H_2 were reacted as above, but with the use of a naphthalene filter solution and photolysis time of 72 h. This procedure gave clusters **3** and **4** as the only products in 100% yield, as indicated by the ^{1}H NMR spectrum of the product mixture. Purification as described above gave isolated **3** and **4** in 12% and 74% yields, respectively.

Crystallographic Structural Determinations of 3 and 4. The crystals were selected under ambient conditions. The crystal data collection was performed on a Bruker CCD-1000 diffractometer with Mo Kα (λ = 0.71073 Å) radiation and a detector-to-crystal distance of 5.03 cm. The data were collected using the full sphere routine and were corrected for Lorentz and polarization effects. The absorption correction was based on fitting a function to the empirical transmission surface as sampled by multiple equivalent measurements using SADABS software.[26]

Positions of the heavy atoms were found by the Patterson method. The remaining atoms were located in an alternating series of least-squares cycles and difference Fourier maps. All non-hydrogen atoms were refined in full-matrix anisotropic approximation. All hydrogen atoms were placed in the structure factor calculation at idealized positions and refined using a "riding" model. Results of the X-ray structure determinations are collected in Table 1.

Acknowledgment. This work was supported by the National Science Foundation through Grant No. CHE-9816342.

Supporting Information Available: PDF and CIF files and tables giving crystallographic data for **3** and **4**, including atomic coordinates, bond lengths and angles, and anisotropic displacement parameters. This material is available free of charge via the Internet at http://pubs.acs.org.

OM0303247

(26) Blessing, R. H. *Acta Crystallogr.* **1995**, *A51*, 33.